


Article

(S)-N-Benzyl-1-phenyl-3,4-dihydroisoquinoline-2(1H)-carboxamide Derivatives, Multi-Target Inhibitors of Monoamine Oxidase and Cholinesterase: Design, Synthesis, and Biological Activity

Qing-Hao Jin ^{1,†}, Li-Ping Zhang ¹, Shan-Shan Zhang ^{2,†}, Dai-Na Zhuang ¹, Chu-Yu Zhang ¹, Zhou-Jun Zheng ^{1,*} and Li-Ping Guan ^{2,*} 

¹ College of Nursing, Zhejiang Pharmaceutical University, Ningbo 315153, China

² Food and Pharmacy College, Zhejiang Ocean University, Zhoushan 316022, China

* Correspondence: zhengzj_good@126.com (Z.-J.Z.); glp730@zjou.edu.cn (L.-P.G.)

† These authors contributed equally to this work.

Abstract: A series of (S)-1-phenyl-3,4-dihydroisoquinoline-2(1H)-carboxamide derivatives was synthesized and evaluated for inhibitory activity against monoamine oxidase (MAO)-A and-B, acetylcholine esterase (AChE), and butyrylcholine esterase (BChE). Four compounds (**2i**, **2p**, **2t**, and **2v**) showed good inhibitory activity against both MAO-A and MAO-B, and two compounds (**2d** and **2j**) showed selective inhibitory activity against MAO-A, with IC₅₀ values of 1.38 and 2.48 μM, respectively. None of the compounds showed inhibitory activity against AChE; however, 12 compounds showed inhibitory activity against BChE. None of the active compounds showed cytotoxicity against L929 cells. Molecular docking revealed several important interactions between the active analogs and amino acid residues of the protein receptors. This research paves the way for further study aimed at designing MAO and ChE inhibitors for the treatment of depression and neurodegenerative disorders.

Keywords: 3,4-dihydroisoquinoline; carboxamide derivatives; monoamine oxidase; cholinesterase; cytotoxicity; molecular docking



Citation: Jin, Q.-H.; Zhang, L.-P.; Zhang, S.-S.; Zhuang, D.-N.; Zhang, C.-Y.; Zheng, Z.-J.; Guan, L.-P. (S)-N-Benzyl-1-phenyl-3,4-dihydroisoquinoline-2(1H)-carboxamide Derivatives, Multi-Target Inhibitors of Monoamine Oxidase and Cholinesterase: Design, Synthesis, and Biological Activity. *Molecules* **2023**, *28*, 1654. <https://doi.org/10.3390/molecules28041654>

Academic Editor: Antonio Massa

Received: 31 December 2022

Revised: 28 January 2023

Accepted: 2 February 2023

Published: 9 February 2023



Copyright: © 2023 by the authors. Licensee MDPI, Basel, Switzerland. This article is an open access article distributed under the terms and conditions of the Creative Commons Attribution (CC BY) license (<https://creativecommons.org/licenses/by/4.0/>).

1. Introduction

Monoamine oxidase (MAO) and cholinesterase (ChE) play important roles in the regulation of nerve conduction by catalyzing the degradation of neurotransmitters. Along with abnormal protein aggregation, low neurotransmitter levels are associated with neuron death [1–3]. Alzheimer's disease (AD) is a common neurodegenerative disease characterized by low levels of the neurotransmitters acetylcholine (ACh) and butyrylcholine (BCh), both of which are involved in cognition. Although multiple hypotheses have been proposed, the exact mechanism of AD development remains elusive; however, the cholinergic hypothesis offers the best explanation to date [4,5]. Clinical treatment of AD involves enhancing cholinergic function by prolonging the usability of ACh that is released into the synaptic space of neurons; this can be achieved by using ChE inhibitors, which inhibit the enzyme responsible for the degradation of ACh. The inhibition of acetylcholinesterase (AChE) and butyrylcholinesterase (BChE) is considered to be beneficial in the treatment of AD [6–9].

Late-life depression (defined as depression in individuals aged sixty years and older) and neurodegenerative disorders, such as AD, are often related and may have a common underlying cause. Depression is a prodromal symptom and risk factor for AD, and may affect up to 50% of symptomatic AD patients [10–12]. MAO is responsible for degrading monoamine neurotransmitters through oxidative deamination. Low levels of monoamine neurotransmitters have been reported to be involved in various pathological processes, including depression and neurodegeneration [13,14]. Elevated MAO levels have been reported as a biomarker in AD patients. It has been hypothesized that elevated MAO levels

induce excessive production of hydroxyl radicals in the brain, triggering a biochemical cascade that is associated with beta-amyloid plaque deposition [15–18]. Furthermore, diverse pharmacological studies have shown that MAO inhibitors have neuroprotective activity associated with the relief of oxidative stress through the regulation of mitochondrial dysfunction [19].

In recent years, the “one molecule, one target” model of drug development has been shown to be inadequate for multi-factorial diseases, especially AD and depression. In light of this, emerging multi-target directed ligands (MTDLs) are promising candidates for the treatment of multi-factorial diseases [20,21]. Ramsay et al. [22] showed that AChE, BChE, MAO-A, and MAO-B are suitable targets for MTDLs. Therefore, ChE and MAO inhibitors have the appropriate properties for the development of MTDLs as neuroprotective and symptomatic drugs and for modulating amyloidogenic pathways.

Isoquinolines and isoquinoline alkaloids are types of plant nitrogen metabolites that have important pharmacological effects, including inhibitory effects against AChE, BChE, MAO-A, MAO-B, and beta-amyloid aggregation [23–25]. Wan Othman et al. [26] have reported that reticuline and nornantenine, which were isolated from the bark of *Cryptocarya griffithiana* Wight, were moderate inhibitors of BChE, with IC_{50} values of 65.04 and 94.45 μ M, respectively. Baek et al. [27] have reported that chelerythrine potently and selectively inhibited MAO-A, with IC_{50} values of 0.55 μ M for MAO-A and > 20.0 μ M for MAO-B. Avicine, which was isolated from a root extract of *Zanthoxylum rigidum* spp. by Gonzalez et al. [28], displayed good inhibitory activity against ChE enzymes and MAO-A, with IC_{50} values of 0.15 μ M electric eel acetylcholinesterase (*Ee*AChE), 0.88 μ M horse serum butyrylcholinesterase (*Eq*BChE), and 0.41 μ M (MAO-A). These results suggested that avicine may be a promising MTDL candidate for the development of new therapeutic agents against AD (Figure 1). In addition, there are clinically approved MAO and ChE inhibitors with carboxamide groups, including moclobemide, toloxatone, and rivastigmine (Figure 1).

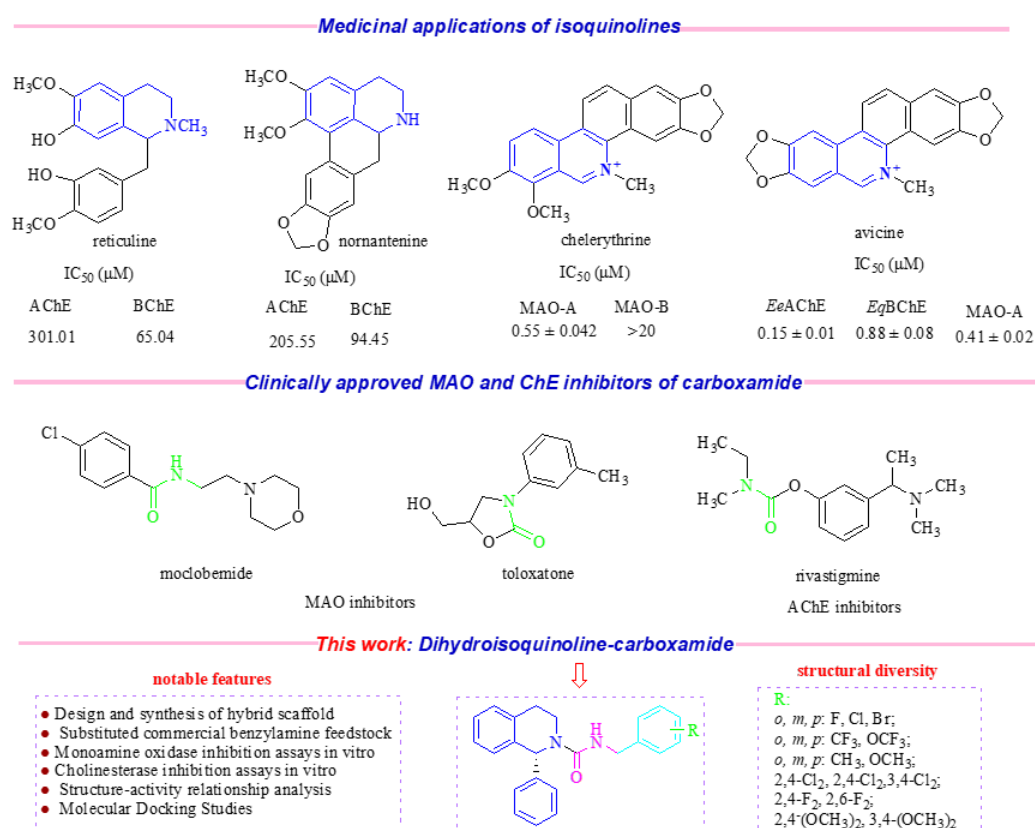


Figure 1. Examples of marketed drugs used for the treatment of AD and depression, and SAR generation around Isoquinolines.

Recently, our research group has reported the preparation of a series of 3,4-dihydroisoquinoline-2(1H)-carboxamide analogs as candidate antidepressant agents. The compound (S)-N-benzyl-1-phenyl-3,4-dihydroisoquinoline-2(1H)-carboxamide (BPIQC) displayed the highest antidepressant effect in the forced swimming test (duration of immobility: 11.0 ± 7.1 s, $p < 0.001$) [29]. Because of our continued interest in the development of dihydroisoquinoline-2(1H)-carboxamide analogs for the treatment of AD and depression, the aim of the present study was to explore the synthesis of a series of (S)-1-phenyl-3,4-dihydroisoquinoline-2(1H)-carboxamide analogs with different N-benzyl substituents using BPIQC as the lead compound. We discuss the potential of the target compounds as inhibitors of AChE, BChE, MAO-A, and MAO-B. In addition, we report a structure–activity relationship (SAR) study of the derivatives, in which the compounds were assessed for cytotoxicity using the 3-(4,5-dimethylthiazol-2-yl)-2,5-diphenyltetrazolium bromide (MTT) assay and acridine orange (AO) fluorescent staining. Molecular docking was used to elucidate the binding modes of the inhibitors.

2. Results and Discussion

2.1. Design of Analogs

The designed molecules consist of three basic components: (i) an isoquinoline ring, which is a major contributor to π – π stacking; (ii) an acyclic carboxamide moiety possessing a nitrogen atom and oxygen atom that can act as forming hydrogen bond donor/acceptor sites for building important interactions with the amino acid residues at the active sites of the enzymes; (iii) a basic foundation of carboxamide-fragment-linked benzyl: recently, our research group found that compound BPIQC displayed the highest antidepressant effect with carboxamide-fragment-linked benzyl [29], in which designing idea is to link the benzyl of donepezil and carboxyl amide of moclobemide together (Figure 2). Therefore, the concept of hybridization not only provides a new and diversified lead structure, but also markedly maintains the pharmacokinetic parameters. Therefore, all kinds of dynamic SAR analyses can be performed to describe the impact of substituent or functional group changes on biological potential.

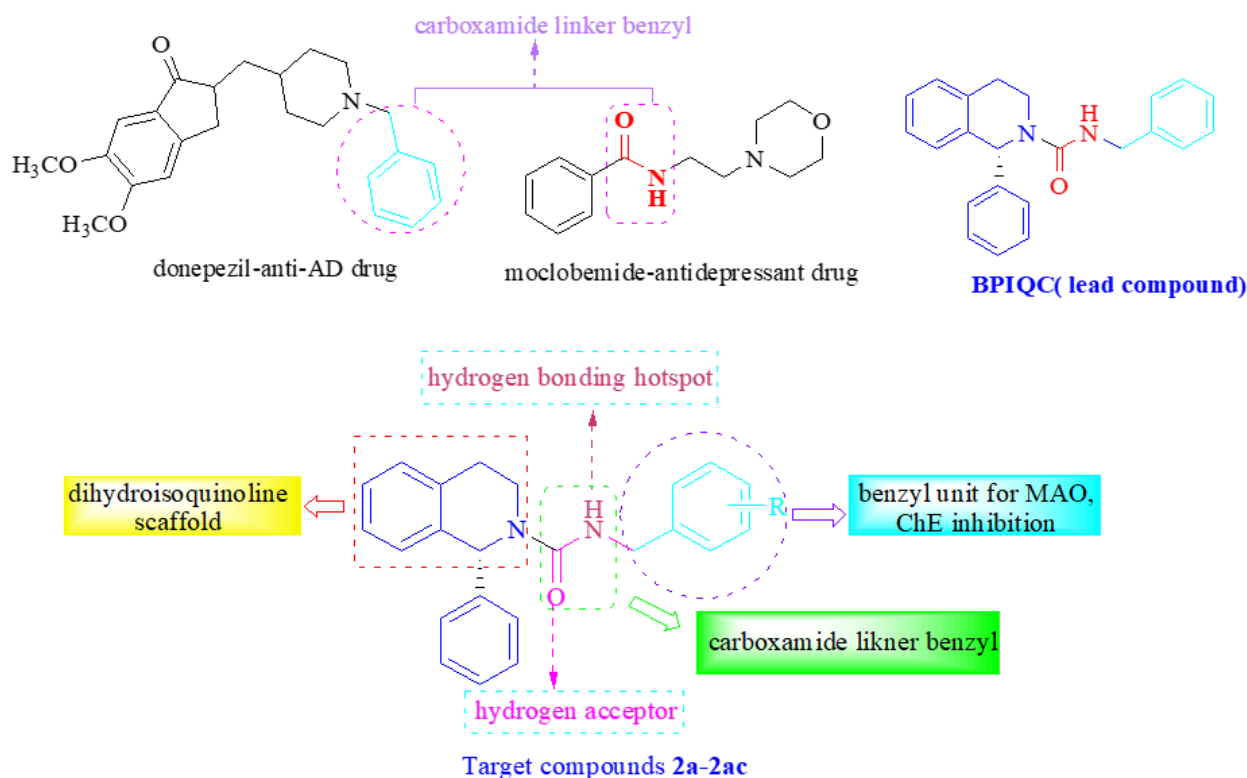
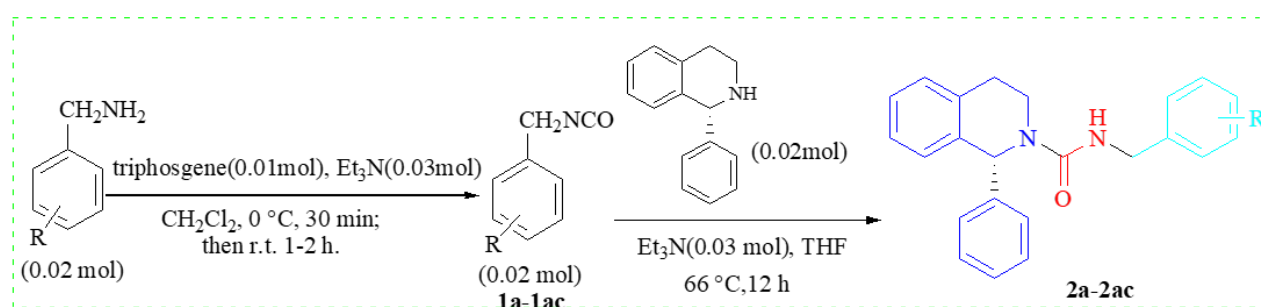


Figure 2. Design strategy for new target compounds 2a–2ac.

2.2. Synthetic Chemistry

A family of (*S*)-1-phenyl-3,4-dihydroisoquinoline-2(1*H*)-carboxamides containing *N*-benzyl substituents was synthesized using a simple route, as shown in Scheme 1. Substitution reactions of commercially available benzylamine with different substituents produced the substituted isocyanates **1a–1ac**, which underwent nucleophilic substitution reactions using triphosgene in 70–85% yield. Subsequently, the substituted isocyanates were condensed with (*S*)-1-phenyl-1,2,3,4-tetrahydroisoquinoline under triethylamine catalysis to afford the desired target compounds **2a–2ac**. Structural characterization and purity determination of the compounds were performed using FT-IR, ¹H-NMR, ¹³C-NMR, ESI-HRMS, and HPLC. (see Supplementary Materials)



R:

1a,2a =H	1b,2b = <i>o</i> -F	1c,2c = <i>m</i> -F	1d,2d = <i>p</i> -F	1e,2e = <i>o</i> -Cl	1f,2f = <i>m</i> -Cl
1g,2g = <i>p</i> -Cl	1h,2h = <i>o</i> -Br	1i,2i = <i>m</i> -Br	1j,2j = <i>p</i> -Br	1k,2k = <i>o</i> -CF ₃	1l,2l = <i>m</i> -CF ₃
1m,2m = <i>p</i> -CF ₃	1n,2n = <i>o</i> -OCF ₃	1o,2o = <i>p</i> -OCF ₃	1p,2p = <i>o</i> -CH ₃	1q,2q = <i>m</i> -CH ₃	1r,2r = <i>p</i> -CH ₃
1s,2s = <i>o</i> -OCH ₃	1t,2t = <i>m</i> -OCH ₃	1u,2u = <i>p</i> -OCH ₃	1v,2v =2,4-(OCH ₃) ₂	1w,2w =3,4-(OCH ₃) ₂	1x,2x =2,4-Cl ₂
1y,2y =2,6-Cl ₂	1z,2z =3,4-Cl ₂	1aa,2aa =2,4-F ₂	1ab,2ab =2,6-F ₂	1ac,2ac = <i>p</i> -CN	

Scheme 1. Synthetic route of derivatives **2a–2ac**.

2.3. Spectroscopic Characterization

The peaks of benzene ring protons, relying on their chemical environment, appeared at approximately 6.82–7.56 ppm. The C-NH signal emerged comparatively upfield as a triplet ($J = 9.0$ Hz or $J = 6.0$ Hz) in the compounds. The triplet spin multiplicity of the –NH peak is ascribed to the coupling of this proton possessing –CH₂ protons in its immediate vicinity. The upfield chemical shift may be considered to be the alkyl carbon atom succeeding –NH that shields the proton [8]. The methine group linked to the benzene ring proton (Ph-CH) displayed an independent single peak downfield at 6.3–6.4 ppm. The ¹³C-NMR spectra further proved the new structures by the presence of a C=O carbon peak at approximately 157.31–162.61 ppm and the presence of signals for the 1,2,3,4-tetrahydroisoquinoline ring carbon atoms (for compound **2v**, these appeared at 28.36 (CH₂), 40.16 (NCH₂), 40.76 (NCH₂CH₂), and 57.88 (Ph-CH) ppm (Figure 3).

2.4. In Vitro Biological Evaluation

2.4.1. Inhibitory Activity of Compounds **2a–2ac** on MAO

The newly prepared (*S*)-1-phenyl-3,4-dihydroisoquinoline carboxamide derivatives **2a–2ac** were tested for inhibitory activity against MAO-A and MAO-B enzymes. First, a preliminary concentration screen of the 29 derivatives **2a–2ac** was conducted (Table 1). Nineteen compounds exhibited inhibitory activity against MAO, with inhibition rates ranging from 29.2 to 71.8% at 100 μM. Among them, six compounds (**2d**, **2i**, **2j**, **2p**, **2t**, and **2v**) showed inhibition rates of more than 50% (52.0–71.8%), and compound **2d**, with a

para-F substituent, displayed the highest inhibitory activity at 71.8%. Next, six compounds (**2d**, **2i**, **2j**, **2p**, **2t**, and **2v**) were chosen for the determination of IC_{50} values. Derivatives **2i**, **2p**, **2t**, and **2v**, incorporating *meta*-Br, *ortho*-CH₃, *meta*-OCH₃, and 2,4-(OCH₃)₂ groups on the benzyl ring, respectively, effectively inhibited both MAO-A and MAO-B; however, their inhibitory activities were lower than that of the drug Rasagiline. In contrast, compounds **2d** and **2j**, with *para*-F and *para*-Br groups on the benzyl ring, respectively, selectively inhibited MAO-A, with IC_{50} values of 1.38 and 2.48 μ M, respectively. Selective MAO-A inhibitors are suitable for the treatment of anxiety and depression [30], whereas MAO-B inhibitors are suitable for the treatment of Parkinson's disease (PD) and AD [31]. Many selective inhibitors for MAO-A and MAO-B have been reported, and some are now used to treat neurological disorders in the clinic [32,33].

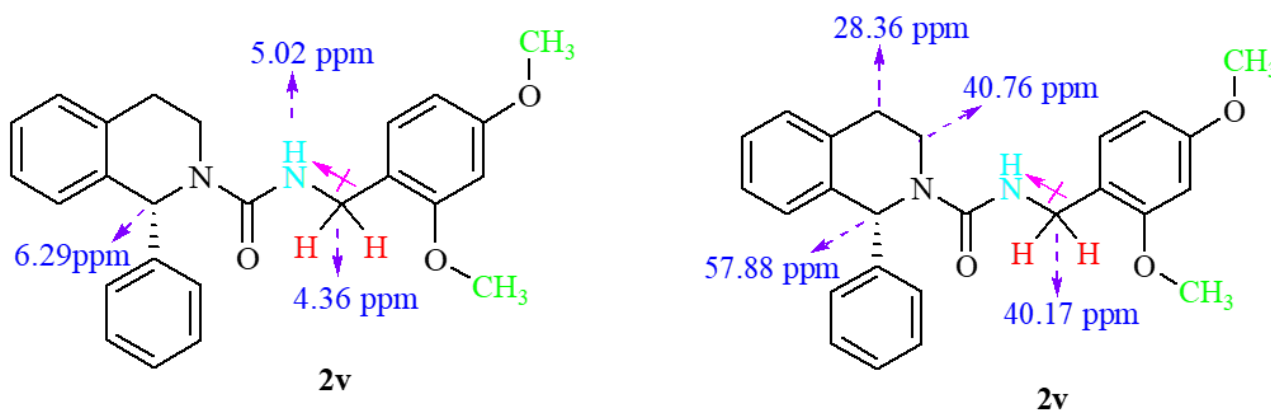


Figure 3. Upfield shifting and splitting of signal in compound **2v**.

2.4.2. In Vitro Cholinesterase Inhibition of Compounds **2a–2ac**

Carboxamide compounds **2a–2ac** were screened for their ability to inhibit AChE and BChE in vitro using Ellman's method (Table 2) [34]. Donepezil and tacolin were used as positive controls. None of the compounds showed inhibitory effects against AChE; however, 12 compounds showed inhibitory effects against BChE. Compound **2t**, with a *meta*-methoxy substituent, was the most potent in the assay, with a BChE inhibition rate of 55% at 100 μ M. This inhibition rate was less potent than the drug tacolin (inhibition rate: 98.2% at 100 μ M). Compounds **2b** (with *ortho*-F) and **2l** (with *meta*-CF₃) also displayed good inhibitory activity, with inhibition rates of 49.0% and 49.1%, respectively. The inhibition of ChE enzymes, namely AChE and BChE, which catalyze the hydrolysis of cholinergic neurotransmitters, may increase the levels of ACh and BCh, respectively, and remains a promising strategy for the treatment of AD [35].

2.5. Cellular Toxicity

Toxicity is a major cause of compound failure at all stages of the drug development process. Most safety-related attrition occurs in the preclinical phase; therefore, safety should be predicted as early as possible during preclinical drug development. This strategy enables the design or selection of improved drug candidates that have a greater chance of becoming commercialized drugs [36]. For this reason, six derivatives with good inhibitory activity (**2d**, **2i**, **2j**, **2p**, **2t**, and **2v**) were tested for cytotoxicity. The results of the MTT cytotoxicity test are shown in Figure 4. Compared with the blank control, six compounds had a viability of more than 90%, and no obvious cytotoxicity was observed from 3.125 to 100 μ M. Thus, **2d**, **2i**, **2j**, **2p**, **2t**, and **2v** have potential as drug candidates. The results of the MTT assay and AO fluorescence staining experiment were confirmed as shown in Figure 5, all six compounds showed no significant toxicity toward L929 cells at 100 μ M, compared with the control group (multiples are 4 \times , 10 \times , and 20 \times).

Table 1. Inhibitory activity (%) of compounds **2a–2ac** against MAO and IC₅₀ values of **2d**, **2i**, **2j**, **2p**, **2t**, and **2v** against MAO-A and MAO-B enzymes.

Compds	Inhibition Rate for MAO ^a (%)	IC ₅₀ (μM)		
		MAO	MAO-A	MAO-B
2a	29.2	- ^c	-	-
2b	N.A. ^b	-	-	-
2c	N.A.	-	-	-
2d	71.8	5.78	1.38	>100
2e	41.4	-	-	-
2f	24.5	-	-	-
2g	21.2	-	-	-
2h	N.A.	-	-	-
2i	58.5	1.34	1.56	4.30
2j	57.4	1.93	2.48	>100
2k	33.0	-	-	-
2l	N.A.	-	-	-
2m	35.8	-	-	-
2n	33.0	-	-	-
2o	31.1	-	-	-
2p	59.4	0.774	2.92	3.88
2q	N.A.	-	-	-
2r	N.A.	-	-	-
2s	N.A.	-	-	-
2t	53.7	2.08	2.50	1.61
2u	N.A.	-	-	-
2v	52.0	0.958	3.51	3.52
2w	N.A.	-	-	-
2x	44.7	-	-	-
2y	37.7	-	-	-
2z	7.40	-	-	-
2aa	32.1	-	-	-
2ab	33.0	-	-	-
2ac	N.A.	-	-	-
Rasagiline	91.75	0.338	0.64	0.97

^a Compounds concentration 100 μM; ^b N.A.—not active; ^c—not test.

Table 2. Inhibitory activity (%) of part compounds against AChE and BChE.

Compds	R	Inhibition Rate ^a (%)	
		AChE	BChE
2b	<i>o</i> -F	N.A. ^b	49.0
2f	<i>m</i> -Cl	N.A.	3.4
2j	<i>p</i> -Br	N.A.	34.5
2l	<i>m</i> -CF ₃	N.A.	49.1
2q	<i>m</i> -CH ₃	N.A.	8.7
2s	<i>o</i> -OCH ₃	N.A.	39.6
2t	<i>m</i> -OCH ₃	N.A.	55.0
2u	<i>p</i> -OCH ₃	N.A.	40.7
2w	3,4-(OCH ₃) ₂	N.A.	9.4
2z	3,4-Cl ₂	N.A.	12.1
2ab	2,6-F ₂	N.A.	24.9
2ac	<i>p</i> -CN	N.A.	17.7
donepezil	-	62.7	- ^c
tacolin	-	-	98.2

^a Compounds concentration 100 μM; ^b N.A.—not active; ^c—not test.

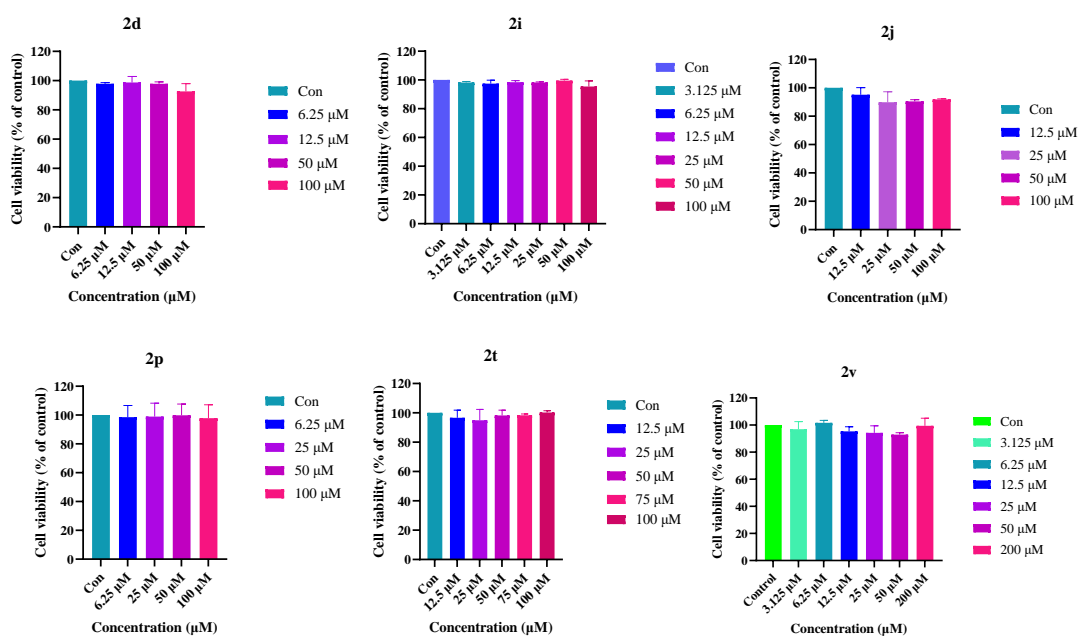


Figure 4. Cytotoxicity of 2d, 2i, 2j, 2p, 2t and 2v on the proliferation of L929 cells (MTT method).

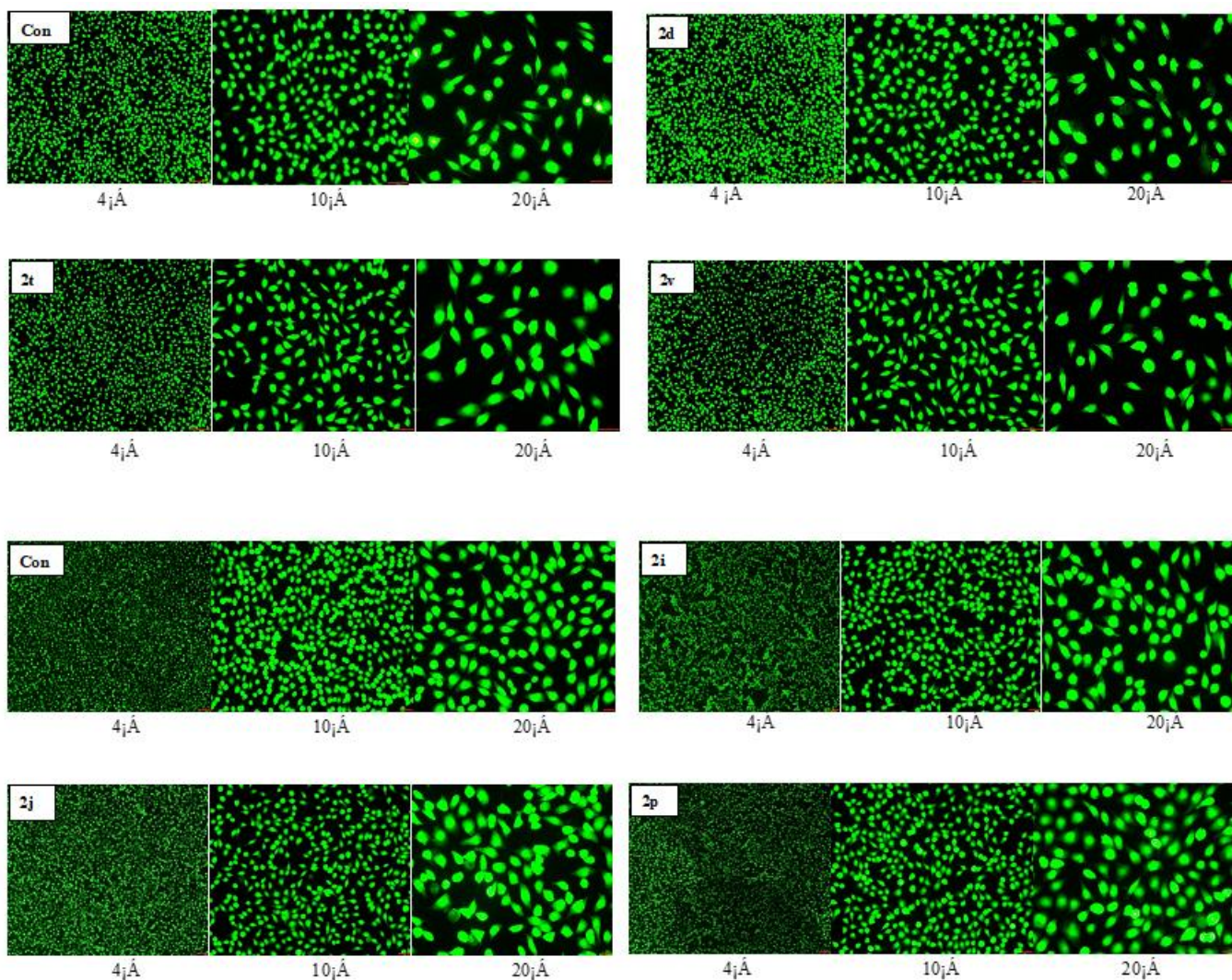


Figure 5. Cytotoxicity of 2d, 2i, 2j, 2p, 2t, and 2v on AO fluorescence staining.

2.6. Molecular Docking Test

Molecular modeling was performed using the Vina (Simina) docking program to further investigate the interaction mode of compound **2t** with MAO-A and MAO-B. Compound **2t**, which displays good MAO-A and MAO-B inhibitory activity, was selected for the molecular docking study. The interaction modes of **2t** with MAO-A and MAO-B revealed that **2t** binds to the active sites of MAO-A and MAO-B, occupying the entire enzymatic catalytic active site (CAS), mid-gorge site, and a peripheral anionic site (PAS) [37]. The docking energies of **2t** were determined to be -9.7 and -8.17 kcal/mol against MAO-A and MAO-B, respectively, as shown in Figure 6 (left: MAO-A, right: MAO-B). The cognate ligand showed conventional hydrogen bonds with Ile23 and a π - π T-shape with the phenyl ring of Tyr407 in the active site of MAO-A. However, a strong hydrogen bond was also formed between the oxygen atom of the carbonyl group of the amide bond and Ser59 and Tyr60 in the active site of MAO-B. These results suggested that compound **2t** is a dual inhibitor of MAO-A and MAO-B, which is consistent with the results obtained from previous analyses.

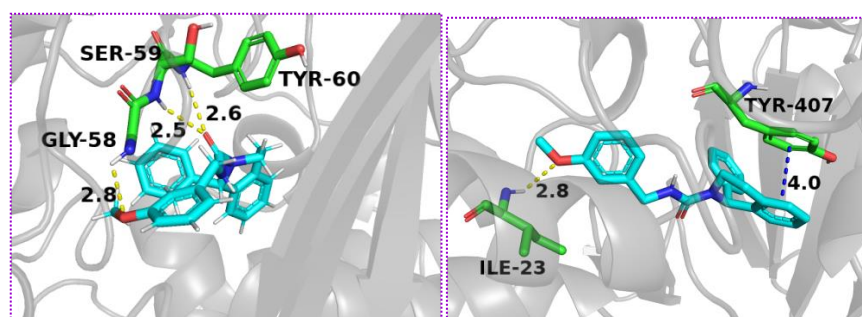


Figure 6. Docking result of **2t** and MAO-A (left), MAO-B (right) (PDB:2Z5X).

3. Experimental Protocols

3.1. Reagents and Instruments

The main chemical agents are bought from Aldrich Chemical Corporation (Shanghai, China). Infrared spectra (IR in KBr) were taken note of for FT-IR1730 (Bruker, Switzerland). The nuclear magnetic resonance spectrum was detected on an AV-300 (Bruker, Switzerland). The shift of chemistry was provided with ppm related to tetramethylsilane. Mass spectra (MS) were detected through ESI-HRMS (Brook Dalton Instruments, Germany). The absorbance value of each good sample was detected on the Epoch 2 microplate reader. HPLC is detected by 1220 Infinity IILC (Agilent Technologies, Santa Clara, CA, USA). An Agilent liquid chromatograph was used to detect its purity. Column temperature: $35\text{ }^{\circ}\text{C}$, detection wavelength: 204 nm, mobile phase: methanol: water (V:V, 82:18), chromatographic column: DIAMONSILTM C₁₈ column (250 mm \times 4.6 mm, 5 μm).

3.2. Synthesis of the Compounds

3.2.1. Preparation of Substituted 1-(Isocyanatomethyl)benzene (**1a–1ac**)

To a stirred solution of triphosgene (0.01 mol) in dry dichloromethane was slowly added a solution of substituted benzylamine (0.02 mol) and triethylamine (0.03 mol) in dichloromethane at $0\text{ }^{\circ}\text{C}$. The resulting mixture was stirred at $0\text{ }^{\circ}\text{C}$ for 30 min, then at room temperature for 1–2 h (reaction progress was monitored by TLC), and the mixture was concentrated into a residue to give intermediates **1a–1ac**. Compounds were purified by recrystallization with EtOH. The yield was 74–91% [38].

3.2.2. Preparation of 3,4-Dihydroisoquinoline Carboxamide Derivatives **2a–2ac**

To a stirred solution of **1a–1ac** (0.02 mol) and triethylamine (0.03 mol) in dry tetrahydrofuran was slowly added (*S*)-1-phenyl-1,2,3,4-tetrahydroisoquinoline (0.02 mol), and the resulting mixture was stirred at $66\text{ }^{\circ}\text{C}$ for 12 h (reaction progress was monitored by TLC).

The mixture was then filtered, and the filtrate was concentrated to a residue, which was purified by silica gel column chromatography/recrystallization to give target compounds **2a–2ac** (Scheme 1) [39].

3.3. Spectral Data of 3,4-Dihydroisoquinoline Carboxamide Derivatives **2a–2ac**

(S)-N-benzyl-1-phenyl-3,4-dihydroisoquinoline-2(1H)-carboxamide (**2a**)

HPLC/Purity: 97.4068% ($t_R = 7.061$), Yield: 41%. mp: 122.5–123.7 °C. IR (KBr) cm^{-1} : 3330, 1610, 1532, 1288. ^1H NMR(CDCl_3 , 300 MHz): δ 7.16–7.32 (m, 14H, C_6H_5), 6.37 (s, 1H, CH), 4.81 (t, $J = 9.0$ Hz, 1H, NH), 4.47 (d, $J = 9.0$ Hz, 2H, N- CH_2), 3.62–3.63 (2H, m, CH_2), 2.79–2.93 (2H, m, CH_2); ^{13}C NMR (CDCl_3 , 75 MHz): δ 157.44, 142.77, 139.42, 136.50, 135.06, 128.62, 128.50, 128.40, 128.25, 127.66, 127.50, 127.27, 127.18, 126.41, 57.90, 45.14, 40.22, 28.38. ESI-MS calcd for $\text{C}_{23}\text{H}_{22}\text{N}_2\text{O}^+$ ($[\text{M} + \text{H}]^+$): 343.1732; found: 343.1720.

(S)-N-(o-fluorobenzyl)-1-phenyl-3,4-dihydroisoquinoline-2(1H)-carboxamide (**2b**)

HPLC/Purity: 93.3234% ($t_R = 7.097$), Yield: 54%. IR (KBr) cm^{-1} : 3302, 1613, 1534, 1220. ^1H NMR(CDCl_3 , 300 MHz): δ 6.98–7.30 (m, 13H, C_6H_5), 6.33 (s, 1H, CH), 4.94 (t, $J = 9.0$ Hz, 1H, NH), 4.49 (d, $J = 9.0$ Hz, 2H, N- CH_2), 3.59–3.62 (m, 2H, CH_2), 2.80–2.88 (m, 2H, CH_2); ^{13}C NMR (CDCl_3 , 75 MHz): δ 162.04, 160.09, 157.43, 142.70, 136.50, 135.02, 130.22, 129.95, 128.92, 128.48, 128.37, 128.21, 127.41, 127.24, 127.17, 126.38, 124.25, 115.32, 115.23, 57.85, 40.15, 39.13, 28.34. ESI-MS calcd for $\text{C}_{23}\text{H}_{21}\text{FN}_2\text{O}^+$ ($[\text{M} + \text{H}]^+$): 361.1638; found: 361.1619.

(S)-N-(m-fluorobenzyl)-1-phenyl-3,4-dihydroisoquinoline-2(1H)-carboxamide (**2c**)

HPLC/Purity: 98.7453% ($t_R = 7.089$), Yield: 55%. IR (KBr) cm^{-1} : 3334, 1612, 1526, 1240. ^1H NMR(CDCl_3 , 300 MHz): δ 6.90–7.29 (m, 13H, C_6H_5), 6.34 (s, 1H, CH), 4.90 (t, $J = 9.0$ Hz, 1H, NH), 4.43 (d, $J = 9.0$ Hz, 2H, N- CH_2), 3.63–3.65 (m, 2H, CH_2), 2.81–2.90 (m, 2H, CH_2); ^{13}C NMR (CDCl_3 , 75 MHz): δ 163.88, 161.79, 157.42, 142.73, 142.19, 136.28, 135.01, 130.07, 128.56, 128.40, 128.20, 127.39, 127.35, 127.21, 126.45, 122.98, 122.96, 114.37, 113.97, 57.97, 44.50, 40.24, 28.42. ESI-MS calcd for $\text{C}_{23}\text{H}_{21}\text{FN}_2\text{O}^+$ ($[\text{M} + \text{H}]^+$): 361.1638; found: 361.1610.

(S)-N-(p-fluorobenzyl)-1-phenyl-3,4-dihydroisoquinoline-2(1H)-carboxamide (**2d**)

HPLC/Purity: 96.1534% ($t_R = 7.141$), Yield: 47%. IR (KBr) cm^{-1} : 3324, 1616, 1500, 1213. ^1H NMR(CDCl_3 , 300 MHz): δ 6.94–7.27 (m, 13H, C_6H_5), 6.34 (s, 1H, CH), 4.89 (t, $J = 9.0$ Hz, 1H, NH), 4.39 (d, $J = 9.0$ Hz, 2H, N- CH_2), 3.60–3.63 (m, 2H, CH_2), 2.27–2.90 (m, 2H, CH_2); ^{13}C NMR (CDCl_3 , 75 MHz): δ 163.00, 161.05, 157.44, 142.75, 136.42, 135.27, 135.01, 129.23, 129.16, 129.07, 128.50, 128.40, 128.20, 128.04, 127.97, 127.42, 127.28, 126.42, 115.43, 57.87, 44.32, 40.15, 28.37. ESI-MS calcd for $\text{C}_{23}\text{H}_{21}\text{FN}_2\text{O}^+$ ($[\text{M} + \text{H}]^+$): 361.1616; found: 361.1615.

(S)-N-(o-chlorobenzyl)-1-phenyl-3,4-dihydroisoquinoline-2(1H)-carboxamide (**2e**)

HPLC/Purity: 92.0620% ($t_R = 8.123$), Yield: 67%. mp: 145.6–147.0 °C. IR (KBr) cm^{-1} : 3356, 1618, 1532, 1237. ^1H NMR(CDCl_3 , 300 MHz): δ 7.15–7.35 (m, 13H, C_6H_5), 6.32 (s, 1H, CH), 5.07 (t, $J = 9.0$ Hz, 1H, NH), 4.52 (d, $J = 9.0$ Hz, 2H, N- CH_2), 3.63–3.65 (m, 2H, CH_2), 2.79–2.92 (m, 2H, CH_2); ^{13}C NMR (CDCl_3 , 75 MHz): δ 157.38, 142.75, 136.83, 136.49, 135.07, 133.56, 130.30, 129.41, 128.66, 128.52, 128.39, 128.21, 127.43, 127.28, 127.16, 127.04, 126.41, 57.97, 43.05, 40.22, 28.41. ESI-MS calcd for $\text{C}_{23}\text{H}_{21}\text{ClN}_2\text{O}^+$ ($[\text{M} + \text{H}]^+$): 377.1342; found: 377.1344.

(S)-N-(m-chlorobenzyl)-1-phenyl-3,4-dihydroisoquinoline-2(1H)-carboxamide (**2f**)

HPLC/Purity: 90.8954% ($t_R = 8.344$), Yield: 61%. IR (KBr) cm^{-1} : 3358, 1618, 1530, 1233. ^1H NMR(CDCl_3 , 300 MHz): δ 7.10–7.29 (m, 13H, C_6H_5), 6.33 (s, 1H, CH), 4.84 (t, $J = 9.0$ Hz, 1H, NH), 4.42 (d, $J = 9.0$ Hz, 2H, N- CH_2), 3.64–3.66 (m, 2H, CH_2), 2.83–2.90 (m, 2H, CH_2); ^{13}C NMR (CDCl_3 , 75 MHz): δ 157.37, 142.71, 142.68, 136.41, 135.01, 134.44, 129.85, 128.59, 128.52, 128.40, 128.20, 127.55, 127.38, 127.30, 127.22, 127.21, 126.47, 126.44, 125.66, 58.01, 44.48, 40.29, 28.31. ESI-MS calcd for $\text{C}_{23}\text{H}_{21}\text{ClN}_2\text{O}^+$ ($[\text{M} + \text{H}]^+$): 377.1342; found: 377.1349.

(S)-N-(p-chlorobenzyl)-1-phenyl-3,4-dihydroisoquinoline-2(1H)-carboxamide (**2g**)

HPLC/Purity: 95.6916% ($t_R = 8.588$), Yield: 47%. IR (KBr) cm^{-1} : 3346, 1612, 1532, 1230. ^1H NMR(CDCl_3 , 300 MHz): δ 7.13–7.29 (m, 13H, C_6H_5), 6.33 (s, 1H, CH), 4.91 (t, $J = 12.0$ Hz, 1H, NH), 4.42 (d, $J = 12.0$ Hz, 2H, N- CH_2), 3.60–3.64 (m, 2H, CH_2), 2.79–2.89 (m, 2H, CH_2); ^{13}C NMR (CDCl_3 , 75 MHz): δ 157.44, 142.75, 138.12, 136.40, 135.01, 132.94, 128.90, 128.79,

128.68, 128.55, 128.42, 128.27, 128.21, 127.43, 127.33, 127.22, 126.46, 57.94, 44.35, 40.20, 28.41. ESI-MS calcd for $C_{23}H_{21}ClN_2O^+$ ($[M + H]^+$): 377.1342; found: 377.1338.

(*S*)-*N*-(*o*-bromobenzyl)-1-phenyl-3,4-dihydroisoquinoline-2(*1H*)-carboxamide (**2h**)

HPLC/Purity: 97.4021% ($t_R = 8.545$), Yield: 69%. mp: 165.9–166.6 °C. IR (KBr) cm^{-1} : 3357, 1618, 1527, 1237. 1H NMR($CDCl_3$, 300 MHz): δ 7.10–7.52 (m, 13H, C_6H_5), 6.32 (1H, s, CH), 5.12 (t, $J = 9.0$ Hz, 1H, NH), 4.50 (d, $J = 9.0$ Hz, 2H, N- CH_2), 3.63–3.65 (m, 2H, CH_2), 2.80–2.90 (m, 2H, CH_2); ^{13}C NMR ($CDCl_3$, 75 MHz): δ 157.34, 142.75, 138.43, 136.49, 135.08, 132.67, 130.53, 130.51, 128.93, 128.52, 128.39, 128.20, 127.67, 127.43, 127.28, 127.17, 126.42, 123.72, 57.97, 45.33, 40.21, 28.41. ESI-MS calcd for $C_{23}H_{21}BrN_2O^+$ ($[M + H]^+$): 421.0837; found: 421.0832.

(*S*)-*N*-(*m*-bromobenzyl)-1-phenyl-3,4-dihydroisoquinoline-2(*1H*)-carboxamide (**2i**)

HPLC/Purity: 97.5607% ($t_R = 8.877$), Yield: 42%. IR (KBr) cm^{-1} : 3356, 1618, 1528, 1230. 1H NMR($CDCl_3$, 300 MHz): δ 7.13–7.36 (m, 13H, C_6H_5), 6.34 (1H, s, CH), 4.97 (t, $J = 9.0$ Hz, 1H, NH), 4.42 (d, $J = 9.0$ Hz, 2H, N- CH_2), 3.61–3.65 (m, 2H, CH_2), 2.79–2.90 (m, 2H, CH_2); ^{13}C NMR ($CDCl_3$, 75 MHz): δ 157.40, 142.71, 136.41, 135.03, 134.38, 130.44, 130.28, 128.94, 128.70, 128.62, 128.59 (CH), 128.25, 128.22, 127.40, 127.37, 127.34, 127.06, 126.45, 122.65, 57.95, 44.40, 40.23, 28.42. ESI-MS calcd for $C_{23}H_{21}BrN_2O^+$ ($[M + H]^+$): 421.0837; found: 421.0821.

(*S*)-*N*-(*p*-bromobenzyl)-1-phenyl-3,4-dihydroisoquinoline-2(*1H*)-carboxamide (**2j**)

HPLC/Purity: 95.8056% ($t_R = 9.161$), Yield: 54%. IR (KBr) cm^{-1} : 3356, 1617, 1530, 1238. 1H NMR($CDCl_3$, 300 MHz): δ 7.07–7.40 (m, 13H, C_6H_5), 6.33 (s, 1H, CH), 4.95 (t, $J = 9.0$ Hz, 1H, NH), 4.36 (d, $J = 9.0$ Hz, 2H, N- CH_2), 3.63–3.65 (m, 2H, CH_2), 2.78–2.88 (m, 2H, CH_2); ^{13}C NMR ($CDCl_3$, 75 MHz): δ 157.44, 142.75, 138.67, 136.39, 133.81, 131.65, 131.62, 129.27, 128.94, 128.71, 128.62, 128.55, 128.43, 128.26, 127.44, 127.34, 127.22, 126.46, 121.02, 57.93, 44.38, 40.18, 28.41. ESI-MS calcd for $C_{23}H_{21}BrN_2O^+$ ($[M + H]^+$): 421.0837; found: 421.0841.

(*S*)-*N*-(*o*-(trifluoromethyl)benzyl)-1-phenyl-3,4-dihydroisoquinoline-2(*1H*)-carboxamide (**2k**)

HPLC/Purity: 92.1203% ($t_R = 7.958$), Yield: 75%. IR (KBr) cm^{-1} : 3318, 1611, 1537, 1306. 1H NMR($CDCl_3$, 300 MHz): δ 7.17–7.62 (m, 13H, C_6H_5), 6.33 (s, 1H, CH), 4.95 (t, $J = 9.0$ Hz, 1H, NH), 4.63 (d, $J = 9.0$ Hz, 2H, N- CH_2), 3.61–3.64 (m, 2H, CH_2), 2.79–2.92 (m, 2H, CH_2); ^{13}C NMR ($CDCl_3$, 75 MHz): δ 157.31, 142.72, 138.02, 136.45, 132.25, 130.63, 128.52, 128.39, 128.20, 128.07, 127.83, 127.65, 127.39, 127.29, 126.44, 125.96, 125.91, 125.87, 125.68, 123.50, 57.94, 41.53, 40.19, 28.38. ESI-MS calcd for $C_{24}H_{21}F_3N_2O^+$ ($[M + H]^+$): 411.1606; found: 411.1602.

(*S*)-*N*-(*m*-(trifluoromethyl)benzyl)-1-phenyl-3,4-dihydroisoquinoline-2(*1H*)-carboxamide (**2l**)

HPLC/Purity: 91.9704% ($t_R = 8.150$), Yield: 52%. IR (KBr) cm^{-1} : 3326, 1612, 1535, 1312. 1H NMR($CDCl_3$, 300 MHz): δ 7.15–7.53 (m, 13H, C_6H_5), 6.34 (s, 1H, CH), 5.03 (t, $J = 9.0$ Hz, 1H, NH), 4.48 (d, $J = 9.0$ Hz, 2H, N- CH_2), 3.62–3.65 (m, 2H, CH_2), 2.81–2.89 (m, 2H, CH_2); ^{13}C NMR ($CDCl_3$, 75 MHz): δ 157.44, 142.65, 139.22, 136.36, 135.00, 131.23, 130.97, 129.81, 128.77, 128.42, 128.19, 127.39, 127.35, 127.25, 126.47, 125.20, 124.33, 124.06, 124.03, 123.04, 58.00, 44.79, 40.26, 28.40. ESI-MS calcd for $C_{24}H_{21}F_3N_2O^+$ ($[M + H]^+$): 411.1606; found: 411.1612.

(*S*)-*N*-(*p*-(trifluoromethyl)benzyl)-1-phenyl-3,4-dihydroisoquinoline-2(*1H*)-carboxamide (**2m**)

HPLC/Purity: 92.1722% ($t_R = 8.509$), Yield: 64%. IR (KBr) cm^{-1} : 3349, 1617, 1532, 1319. 1H NMR($CDCl_3$, 300 MHz): δ 7.15–7.53 (m, 13H, C_6H_5), 6.33 (s, 1H, CH), 5.01 (t, $J = 9.0$ Hz, 1H, NH), 4.47 (d, $J = 9.0$ Hz, 2H, N- CH_2), 3.66–3.68 (m, 2H, CH_2), 2.80–2.93 (m, 2H, CH_2); ^{13}C NMR ($CDCl_3$, 75 MHz): δ 156.65, 143.77, 141.31, 136.34, 134.66, 128.69, 128.44, 128.25, 128.02, 127.61, 126.97, 126.61, 126.23, 125.17, 124.89, 123.10, 58.74, 43.75, 40.25, 28.02. ESI-MS calcd for $C_{24}H_{21}F_3N_2O^+$ ($[M + H]^+$): 411.1606; found: 411.1611.

(*S*)-*N*-(*o*-(trifluoromethoxy)benzyl)-1-phenyl-3,4-dihydroisoquinoline-2(*1H*)-carboxamide (**2n**)

HPLC/Purity: 94.9895% ($t_R = 8.545$), Yield: 65%. IR (KBr) cm^{-1} : 3301, 1614, 1535, 1248. 1H NMR($CDCl_3$, 300 MHz): δ 7.16–7.39 (m, 13H, C_6H_5), 6.33 (s, 1H, CH), 4.95 (t, $J = 9.0$ Hz,

1H, NH), 4.51 (d, $J = 9.0$ Hz, 2H, N-CH₂), 3.62–3.65 (m, 2H, CH₂), 2.80–2.92 (m, 2H, CH₂); ¹³C NMR (CDCl₃, 75 MHz): δ 157.41, 147.35, 142.72, 136.46, 135.03, 132.01, 130.26, 128.62, 128.52, 128.39, 128.20127.39, 127.29, 127.19, 127.06, 126.43, 121.61, 120.42, 119.57, 57.95, 40.18, 39.68, 28.38. ESI-MS calcd for C₂₄H₂₁F₃N₂O₂⁺ ([M + H]⁺): 427.1555; found: 427.1561.

(S)-N-(*p*-(trifluoromethoxy)benzyl)-1-phenyl-3,4-dihydroisoquinoline-2(1H)-carboxamide(**2o**)

HPLC/Purity: 93.1264% ($t_R = 9.132$), Yield: 57%. IR (KBr) cm⁻¹: 3303, 1612, 1533, 1258. ¹H NMR(CDCl₃, 300 MHz): δ 7.11–7.27 (m, 13H, C₆H₅), 6.34 (s, 1H, CH), 5.00 (t, $J = 9.0$ Hz, 1H, NH), 4.47 (d, $J = 9.0$ Hz, 2H, N-CH₂), 3.62–3.65 (m, 2H, CH₂), 2.81–2.93 (m, 2H, CH₂); ¹³C NMR (CDCl₃, 75 MHz): δ 157.42, 142.73, 138.38, 136.38, 134.99, 128.88, 128.56, 128.42, 128.21, 127.42, 127.35, 127.23, 126.47, 121.19, 121.11, 57.98, 44.26, 40.24, 28.42. ESI-MS calcd for C₂₄H₂₁F₃N₂O₂⁺ ([M + H]⁺): 427.1555; found: 427.5544.

(S)-N-(*o*-methylbenzyl)-1-phenyl-3,4-dihydroisoquinoline-2(1H)-carboxamide (**2p**)

HPLC/Purity: 97.3785% ($t_R = 8.011$), Yield: 57%. mp:125.6–127.3 °C. IR (KBr) cm⁻¹: 3340, 1610, 1524, 1235. ¹H NMR(CDCl₃, 300 MHz): δ 7.03–7.26 (m, 13H, C₆H₅), 6.37 (s, 1H, CH), 4.78 (t, $J = 6.0$ Hz, 1H, NH), 4.42 (d, $J = 6.0$ Hz, 2H, N-CH₂), 3.62–3.63 (m, 2H, CH₂), 2.82–2.89 (m, 2H, CH₂), 2.32 (3H, s, CH₃); ¹³C NMR (CDCl₃, 75 MHz): δ 157.47, 142.83, 139.33, 138.28, 136.53, 135.09, 130.44, 128.51, 128.47, 128.40, 128.38, 128.29, 128.01, 127.47, 127.23, 127.15, 126.39, 126.12, 124.68, 57.83, 45.10, 40.15, 28.39, 21.38. ESI-MS calcd for C₂₄H₂₄N₂O⁺ ([M + H]⁺): 357.1889; found: 357.1872.

(S)-N-(*m*-methylbenzyl)-1-phenyl-3,4-dihydroisoquinoline-2(1H)-carboxamide (**2q**)

HPLC/Purity: 97.9738% ($t_R = 8.001$), Yield: 51%. mp:142.7–144.0 °C. IR (KBr) cm⁻¹: 3346, 1610, 1525, 1240. ¹H NMR(CDCl₃, 300 MHz): δ 7.05–7.27 (m, 13H, C₆H₅), 6.37 (s, 1H, CH), 4.78 (t, $J = 9.0$ Hz, 1H, NH), 4.45 (d, $J = 9.0$ Hz, 2H, N-CH₂), 3.60–3.63 (m, 2H, CH₂), 2.82–2.89 (m, 2H, CH₂), 2.32 (s, 3H, CH₃); ¹³C NMR (CDCl₃, 75 MHz): δ 157.47, 142.83, 139.33, 138.28, 136.53, 135.09, 128.51, 128.47, 128.40, 128.38, 128.23, 128.01, 127.47, 127.23, 127.15, 126.39, 124.68, 57.83, 45.10, 40.15, 28.39, 21.38. ESI-MS calcd for C₂₄H₂₄N₂O⁺ ([M + H]⁺): 357.1889; found: 357.1893.

(S)-N-(*p*-methylbenzyl)-1-phenyl-3,4-dihydroisoquinoline-2(1H)-carboxamide (**2r**)

HPLC/Purity: 94.9442% ($t_R = 7.649$), Yield: 56%. IR (KBr) cm⁻¹: 3356, 1616, 1527, 1248. ¹H NMR(CDCl₃, 300 MHz): δ 7.09–7.26 (m, 13H, C₆H₅), 6.37 (s, 1H, CH), 4.81 (t, $J = 9.0$ Hz, 1H, NH), 4.43 (d, $J = 9.0$ Hz, 2H, N-CH₂), 3.57–3.61 (m, 2H, CH₂), 2.80–2.88 (m, 2H, CH₂), 2.30 (s, 3H, CH₃); ¹³C NMR (CDCl₃, 75 MHz): δ 157.50, 142.84, 136.93, 136.55, 136.41, 135.11, 129.29, 128.47, 128.40, 128.26, 127.70, 127.51, 127.22, 127.16, 126.39, 57.78, 44.91, 40.11, 28.37, 21.10. ESI-MS calcd for C₂₄H₂₄N₂O⁺ ([M + H]⁺): 357.1889; found: 357.1896.

(S)-N-(*o*-methoxybenzyl)-1-phenyl-3,4-dihydroisoquinoline-2(1H)-carboxamid (**2s**)

HPLC/Purity: 97.2296% ($t_R = 7.344$), Yield: 68%. mp:165.5–166.6 °C. IR(KBr)cm⁻¹: 3431, 1638, 1512, 1239. ¹H NMR(CDCl₃, 300 MHz): δ 6.81–7.23 (m, 13H, C₆H₅), 6.31 (s, 1H, CH), 5.14 (t, $J = 6.0$ Hz, 1H, NH), 4.45 (d, $J = 6.0$ Hz, 2H, N-CH₂), 3.76 (s, 3H, OCH₃), 3.60–3.76 (m, 2H, CH₂), 2.72–2.91 (m, 2H, CH₂); ¹³C NMR (CDCl₃, 75 MHz): δ 157.75, 157.56, 142.92, 136.69, 135.27, 129.76, 128.97, 128.57, 128.42, 128.36, 128.19, 127.45, 127.14, 127.11, 126.35, 120.72, 110.23, 57.90, 55.26, 41.17, 40.14, 28.38. ESI-MS calcd for C₂₄H₂₄N₂O₂⁺ ([M + H]⁺): 373.1838; found: 373.1822.

(S)-N-(*m*-methoxybenzyl)-1-phenyl-3,4-dihydroisoquinoline-2(1H)-carboxamide (**2t**)

HPLC/Purity: 96.3463% ($t_R = 6.838$), Yield: 72%. mp: 108.4–109.4 °C. IR (KBr) cm⁻¹: 3342, 1611, 1528, 1257. ¹H NMR(CDCl₃, 300 MHz): δ 6.80–7.26 (m, 13H, C₆H₅), 6.38 (s, 1H, CH), 4.80 (s, 1H, -NH), 4.44 (d, $J = 6.0$ Hz, 2H, N-CH₂), 3.77 (s, 3H, OCH₃), 3.61–3.63 (m, 2H, CH₂), 2.79–2.90 (m, 2H, CH₂); ¹³C NMR (CDCl₃, 75 MHz): δ 159.86, 157.46, 142.78, 141.08, 136.51, 135.06, 129.63, 128.47, 128.39, 128.24, 127.47, 127.24, 127.17, 126.40, 119.86, 113.11, 112.86, 57.81, 55.22, 45.10, 40.16, 28.36. ESI-MS calcd for C₂₄H₂₄N₂O₂⁺ ([M + H]⁺): 373.1838; found: 373.1843.

(S)-N-(*p*-methoxybenzyl)-1-phenyl-3,4-dihydroisoquinoline-2(1H)-carboxamide (**2u**)

HPLC/Purity: 96.9381% ($t_R = 8.111$), Yield: 44%. IR (KBr) cm⁻¹: 3346, 1612, 1526, 1248. ¹H NMR(CDCl₃, 300 MHz): δ 6.06–7.51 (m, 13H, C₆H₅), 6.47 (s, 1H, CH), 6.10 (t,

$J = 6.0$ Hz, 1H, NH), 4.50 (d, $J = 6.0$ Hz, 2H, N-CH₂), 3.77 (s, 3H, OCH₃), 3.49–3.75 (m, 2H, CH₂), 2.72–2.81 (m, 2H, CH₂); ¹³C NMR (CDCl₃, 75 MHz): δ 162.33, 147.70, 141.19, 139.97, 134.45, 133.26, 132.96, 132.42, 131.93, 131.79, 131.75, 130.87, 128.85, 125.32, 119.87, 119.59, 115.31, 61.93, 45.68, 44.29, 43.15, 32.96. ESI-MS calcd for C₂₄H₂₄N₂O₂⁺ ([M + H]⁺): 373.1838; found: 373.1830.

(S)-N-(2,4-dimethoxybenzyl)-1-phenyl-3,4-dihydroisoquinoline-2(1H)-carboxamide (**2v**)

HPLC/Purity: 90.5831% (t_R = 7.378), Yield: 78%. mp: 153.5–155.4 °C. IR (KBr) cm⁻¹: 3345, 1614, 1534, 1201. ¹H NMR(CDCl₃, 300 MHz): δ 6.41–7.26 (m, 12H, C₆H₅), 6.29 (s, 1H, CH), 5.02 (t, $J = 6.0$ Hz, 1H, NH), 4.36 (d, $J = 6.0$ Hz, 2H, N-CH₂), 3.79 (s, 3H, OCH₃), 3.74 (s, 3H, OCH₃), 3.55–3.60 (m, 2H, CH₂), 2.78–2.87 (m, 2H, CH₂); ¹³C NMR (CDCl₃, 75 MHz): δ 160.33, 158.58, 157.73, 130.54, 128.38, 128.33, 128.17, 127.44, 127.10, 127.07, 126.31, 120.03, 103.91, 98.62, 57.88, 55.42, 55.28, 40.76, 40.10, 28.36. ESI-MS calcd for C₂₅H₂₆N₂O₃⁺ ([M + H]⁺): 403.1943; found: 403.1976.

(S)-N-(3,4-dimethoxybenzyl)-1-phenyl-3,4-dihydroisoquinoline-2(1H)-carboxamide (**2w**)

HPLC/Purity: 97.5223% (t_R = 6.851), Yield: 53%. IR (KBr) cm⁻¹: 3335, 1612, 1514, 1216. ¹H NMR(CDCl₃, 300 MHz): δ 6.95–7.26 (m, 12H, C₆H₅), 6.48 (s, 1H, CH), 4.99 (t, $J = 6.0$ Hz, 1H, NH), 4.19 (d, $J = 6.0$ Hz, 2H, N-CH₂), 3.78 (s, 3H, OCH₃), 3.74 (s, 3H, OCH₃), 3.19–3.16 (m, 2H, CH₂), 2.61–2.69 (m, 2H, CH₂); ¹³C NMR (CDCl₃, 75 MHz): δ 158.09, 154.92, 148.97, 148.29, 141.27, 133.60, 130.75, 129.72, 128.01, 127.28, 125.91, 120.32, 119.28, 111.91, 111.23, 58.06, 55.95, 44.79, 40.25, 28.02. ESI-MS calcd for C₂₅H₂₆N₂O₃⁺ ([M + H]⁺): 403.1943; found: 403.1935.

(S)-N-(2,4-dichlorobenzyl)-1-phenyl-3,4-dihydroisoquinoline-2(1H)-carboxamide(**2x**)

HPLC/Purity: 95.9287% (t_R = 11.059), Yield: 64%.mp: 130.8–132.7 °C. IR (KBr) cm⁻¹: 3280, 1612, 1517, 1210. ¹H NMR(CDCl₃, 300 MHz): δ 7.15–7.33 (m, 12H, C₆H₅), 6.28 (s, 1H, CH), 5.10 (s, 1H, -NH), 4.48 (d, $J = 6.0$ Hz, 2H, N-CH₂), 3.63–3.65 (m, 2H, CH₂), 2.79–2.92 (m, 2H, CH₂); ¹³C NMR (CDCl₃, 75 MHz): δ 157.32, 142.66, 136.35, 135.52, 134.98, 134.05, 133.63, 131.03, 129.17, 128.58, 128.42, 128.18, 127.39, 127.26, 127.22, 126.47, 58.10, 42.46, 40.29, 28.42. ESI-MS calcd for C₂₃H₂₀Cl₂N₂O⁺ ([M + H]⁺): 411.0953; found: 411.0958.

(S)-N-(2,6-dichlorobenzyl)-1-phenyl-3,4-dihydroisoquinoline-2(1H)-carboxamide(**2y**)

HPLC/Purity: 98.4243% (t_R = 9.300), Yield: 68%. mp: 169.0–169.4 °C. IR (KBr) cm⁻¹: 3289, 1617, 1527, 1220. ¹H NMR(CDCl₃, 300 MHz): δ 7.13–7.30 (m, 12H, C₆H₅), 6.29 (s, 1H, CH), 4.96 (t, $J = 6.0$ Hz, 1H, NH), 4.74 (d, $J = 6.0$ Hz, 2H, N-CH₂), 3.60–3.64 (m, 2H, CH₂), 2.76–2.91 (m, 2H, CH₂); ¹³C NMR (CDCl₃, 75 MHz): δ 157.16, 142.75, 136.49, 136.14, 135.10, 134.67, 129.28, 128.49, 128.39, 128.21, 127.45, 127.26, 127.11, 126.36, 57.98, 40.72, 40.18, 28.41. ESI-MS calcd for C₂₃H₂₀Cl₂N₂O⁺ ([M + H]⁺): 411.0953; found: 411.0962.

(S)-N-(3,4-dichlorobenzyl)-1-phenyl-3,4-dihydroisoquinoline-2(1H)-carboxamide (**2z**)

HPLC/Purity: 97.6748% (t_R = 10.458), Yield: 67%. mp: 120.1–120.9 °C. IR (KBr) cm⁻¹: 3282, 1615, 1523, 1224 ¹H NMR(CDCl₃, 300 MHz): δ 7.04–7.33 (m, 12H, C₆H₅), 6.31 (s, 1H, CH), 5.03 (s, 1H, NH), 4.41 (d, $J = 9.0$ Hz, 2H, N-CH₂), 3.64–3.67 (m, 2H, CH₂), 2.79–2.92 (m, 2H, CH₂); ¹³C NMR (CDCl₃, 75 MHz): δ 157.35, 142.64, 140.06, 136.30, 134.95, 132.52, 131.06, 130.46, 129.28, 128.64, 128.44, 128.18, 127.44, 127.36, 127.27, 126.81, 126.50, 58.04, 43.87, 40.28, 28.43. ESI-MS calcd for C₂₃H₂₀Cl₂N₂O⁺ ([M + H]⁺): 411.0953; found: 411.0942.

(S)-N-(2,4-difluorobenzyl)-1-phenyl-3,4-dihydroisoquinoline-2(1H)-carboxamide(**2aa**)

HPLC/Purity: 95.3932% (t_R = 7.433), Yield: 47%. IR (KBr) cm⁻¹: 3303, 1612, 1525, 1223. ¹H NMR(CDCl₃, 300 MHz): δ 7.15–7.27 (m, 12H, C₆H₅), 6.31 (s, 1H, CH), 4.97 (t, $J = 9.0$ Hz, 1H, NH), 4.43(d, $J = 9.0$ Hz, 2H, N-CH₂), 3.61–3.64(m, 2H, CH₂), 2.72–2.91 (m, 2H, CH₂); ¹³C NMR (CDCl₃, 75 MHz): δ 163.26, 163.16, 161.98, 161.89, 161.28, 161.19, 159.92, 157.40, 155.04, 142.68, 136.41, 135.01, 128.63, 128.51, 128.40, 128.21, 128.07, 127.40, 127.30, 127.21, 126.58, 111.29, 103.19, 57.90, 39.87, 38.45, 28.69. ESI-MS calcd for C₂₃H₂₀F₂ N₂O⁺ ([M + H]⁺): 379.1544; found: 379.1552.

(S)-N-(2,6-difluorobenzyl)-1-phenyl-3,4-dihydroisoquinoline-2(1H)-carboxamide(**2ab**)

HPLC/Purity: 94.9327% (t_R = 6.820), Yield:71%. mp: 125.3–128.4 °C. IR (KBr) cm⁻¹: 3301, 1615, 1524, 1228. ¹H NMR(CDCl₃, 300 MHz): δ 7.84–7.25 (m, 12H, C₆H₅), 6.32 (s, 1H, CH), 4.92 (s, 1H, -NH), 4.52 (d, $J = 9.0$ Hz, 2H, N-CH₂), 3.58–3.60 (m, 2H CH₂), 2.75–2.90

(m, 2H, CH₂); ¹³C NMR (CDCl₃, 75 MHz): δ 162.61, 162.54, 160.63, 160.57, 157.14, 142.68, 136.49, 135.08, 129.13, 128.44, 128.37, 128.23, 127.45, 127.21, 127.13, 126.36, 115.08, 114.93, 111.33, 57.79, 40.08, 33.13, 28.32. ESI-MS calcd for C₂₃H₂₀F₂N₂O⁺ ([M + H]⁺): 379.1544; found: 379.1548.

(S)-N-(p-cyanobenzyl)-1-phenyl-3,4-dihydroisoquinoline-2(1H)-carboxamide(**2ac**)

HPLC/Purity: 98.0928% (t_R = 5.802), Yield:49%. IR (KBr) cm⁻¹: 3329, 1620, 1526, 1232. ¹H NMR(CDCl₃, 300 MHz): δ 7.16–7.56 (m, 13H, C₆H₅), 6.31 (s, 1H, CH), 5.04 (t, J = 3.0 Hz, 1H, NH), 4.44 (d, J = 3.0 Hz, 2H, N-CH₂), 3.65–3.68 (m, 2H, CH₂), 2.84–2.98 (m, 2H, CH₂); ¹³C NMR (CDCl₃, 75 MHz): δ 157.37, 145.34, 142.66, 136.24, 134.91, 132.40, 132.34, 128.79, 128.69, 128.46, 128.28, 128.07, 127.89, 127.45, 127.39, 127.30, 126.54, 118.86, 110.89, 58.08, 44.50, 40.30, 28.44. ESI-MS calcd for C₂₄H₂₁N₃O⁺ ([M + H]⁺): 368.1685; found: 368.1676.

4. Biological Activity

4.1. MAO Activity Assay

The enzyme activity analysis was performed according to the procedure reported by Matsumoto et al. with slight modifications. All materials used in the enzymatic assays were purchased from Aladdin Reagent Chemicals. A fixed concentration of tyramine substrate and different concentrations of target compounds or inhibitor were used to confirm the percentage inhibition rate or IC₅₀ values. Tyramine concentrations for MAO-A and -B were 120 μM. The concentrations of the synthesized compounds altered from 0.001 μM to 100 μM for the MAO-A and -B enzyme activity inhibition. The compounds **2a–2ac** were dissolved in 2% DMSO, diluted in buffer solution before the test assay, and pre-cultured with the enzyme at 37 °C for 30 min. The final concentration of DMSO in the enzyme-measured reaction mixture did not exceed 1%. The enzymatic reactions were caused by the addition of MAO-A (40 μg/mL) or MAO-B (20 μg/mL), and cultured at 37 °C for 30 min. The enzyme reactions were stopped through the addition of 2N NaOH for 75 μL. Fluorescence was recorded from the top by using the Infinite 200 PRO multimode microplate reader at the excitation or emission wavelengths of 310 and 380 nm, IC₅₀ values using the software Prism 8 program. The inhibitory effect of enzyme activity was calculated as a percentage of product formation compared to the corresponding control with no inhibitor. A control was established to determine the interference of the tested compounds to the fluorescence assay, and the enzyme or substrate was added after the reaction stopped.

4.2. In Vitro Cholinesterase Inhibition Assay

Inhibition of AChE and BChE was measured through the spectrophotometric method developed by Ellman's method with slight modifications [34]. The analysis protocol contained 96-well plates (100 μL per well). Each well involved 20 μL of assay buffer solution, 20 μL of the test sample, and 40 μL of 0.2 U/mL of AChE or BChE. The mixture was incubated for 10 min at 25 °C followed by the addition of substrate (20 μL). For AChE inhibition assay, acetylthiocholine iodide (ATCI, 0.001 mol/L), while for BChE assay, butyrylthiocholine chloride (BTCCL, 0.001 mol/L) was added to it. The mixture was incubated at 37 °C for 15 min. Ellman reagent (5,5'-dithio-bis(2-nitrobenzoic acid), DTNB, 0.001 mol/L) was added. The change in color of the mixture displayed an indication of inhibition. The absorbance was measured at 412 nm using the microplate reader Infinite 200 PRO, Inc. Switzerland. The blank analysis was performed. All the analyses were performed in triplicate. Inhibition rate of experimental sample or positive control group (%) = [(control group-blank background)-(experimental sample or positive control group-sample background)]/(control-blank background) × 100%.

4.3. Cytotoxicity Test

L929 cells in the logarithmic growth phase were selected, and the cell density was adjusted to 2 × 10⁴ per well by a cell counter. The 96-well plate was inoculated in a 96-well plate, and the 96-well plate inoculated with cells was cultured in a 37 °C 5% carbon dioxide cell incubator for 24 h. Then, the medium containing 100 μM of the compound to be tested

was added (the blank group was added to the medium without drug), shaken gently, and placed in a 5% carbon dioxide cell incubator at 37 °C for 24 h. Each concentration was repeated for 6 h.

4.3.1. MTT Assay to Detect Cell Viability

The assay detects live cells, but not dead cells, and the resulting signal depends on how activated the cells are. Since yellow MTT can be reduced to blue-violet formazan by mitochondrial dehydrogenase in living cells, dimethyl sulfoxide can dissolve formazan (Formazan) in cells, and its light absorption value was measured with a microplate reader at a wavelength of 490 nm. Therefore, MTT has been used to establish quantitative colorimetric assays for mammalian cell survival and proliferation. Therefore, this method can be used to measure cytotoxicity, proliferation, or activation. After 24 h, 20 µL of 5 mg/kg MTT solution (prepared in PBS with pH 7.6) was added in the dark, and cultured in a cell incubator for another 4 h. After 4 h, the 96 plate was taken out to discard the original medium, and 160 µL of DMSO was added, placed on a shaker, and mixed for about 10 min. Then, a microplate reader was used to measure its absorbance at 490 nm, and the results were recorded and analyzed.

4.3.2. Analysis of Cell Viability by AO Fluorescent Staining

Using the AO Fluorescent Staining Kit, AO is a tricyclic heteroaromatic dye that can penetrate cells with intact cell membranes and embed nuclear DNA, making them emit bright green fluorescence. L929 cells were selected from the logarithmic growth phase, and the cell density was adjusted to 8×10^5 per well with a cell counter to inoculate in a 6-well plate, and the 6-well plate was placed in a 37 °C 5% carbon dioxide cell incubator for 12 h. It grew completely adhering to the wall. After 12 h, 1 mL of medium containing 100 µM of the compound to be tested was added (for the blank group, drug-free medium was added), shaken gently, and placed in a 5% carbon dioxide cell incubator at 37 °C for 12 h. After 12h, the medium was discarded, PBS was added to wash once, 1 mL of PBS and 80 µL of AO solution (prepared according to the kit instructions) were slowly added in the dark, and mixed for 5 min to make the staining uniform and sufficient. The staining was aspirated after 5 min, washed 1–2 times with PBS, and observed under a fluorescence microscope, the results were recorded and analyzed.

4.4. Molecular Docking Study

Molecular simulations and docking experiments were performed using the Vina (Simina) docking program. The protein crystal structure of human MAO-A was obtained from the Protein Crystal Database (PDB ID: 2Z5X) with a resolution of 5 Å (10–10 m). The initial structure of the MAO-A protein crystal was processed with default parameters, with the pocket being the center of the FAD ligand. Molecular simulation of the optimized protein crystal structure with 3,4-dihydroisoquinolinecarboxamide compounds **2t** and **2d** provides ideas for the design of better MAO-A inhibitors in the future.

5. Conclusions

In recent years, MAO and ChE inhibitors have received increased attention because of their beneficial effects on mental health. For this reason, we designed and prepared a family of (S)-1-phenyl-3,4-dihydroisoquinoline-2(1H)-carboxamide analogs. Six analogs (**2d**, **2i**, **2j**, **2p**, **2t**, and **2v**) showed good inhibitory activities against MAO with inhibition rates from 52.0 to 71.8%. Analog **2i**, **2p**, **2t**, and **2v**, incorporating *m*-Br, *o*-CH₃, *m*-OCH₃, and 2,4-(OCH₃)₂ groups on the benzyl ring, respectively, showed potent inhibitory effects against MAO-A and MAO-B enzymes. Compounds **2d** and **2j** with *p*-F and *p*-Br groups on the benzyl ring, respectively, selectively inhibited MAO-A, with IC₅₀ values of 1.38 and 2.48 µM, respectively. None of the synthesized compounds showed inhibitory activity against AChE, and 12 compounds displayed inhibitory activities against BChE. In addition, the active compounds did not show any cytotoxicity at the dose required for MAO and

ChE inhibition. Our results indicated that **2t** is a potent inhibitor of MAO-A, MAO-B, and BChE enzymes, and could be a promising candidate for preclinical development for the treatment of depression, AD, and PD.

Supplementary Materials: The following supporting information can be downloaded at: <https://www.mdpi.com/article/10.3390/molecules28041654/s1>, HPLC Data of Derivatives (**2d**, **2i**, **2j**, **2p**, **2t**, and **2v**); NMR data of derivatives **2a–2ac**).

Author Contributions: Conceptualization, L.-P.G. and Z.-J.Z.; data curation, Q.-H.J. and D.-N.Z.; formal analysis, Q.-H.J.; funding acquisition, L.-P.G.; investigation, Z.-J.Z.; methodology, L.-P.G. and Q.-H.J.; project administration, L.-P.G.; resources, L.-P.Z.; software, S.-S.Z., D.-N.Z. and C.-Y.Z.; validation, L.-P.G., Z.-J.Z. and Q.-H.J.; visualization, L.-P.G.; writing—original draft, Q.-H.J. and Z.-J.Z.; writing—review and editing, L.-P.G. All authors have read and agreed to the published version of the manuscript.

Funding: This research received no external funding.

Institutional Review Board Statement: This study was carried out in strict accordance with the recommendations in the Guide for the Care and Use of Laboratory Animals of the National Institutes of Health. The protocol was approved by the Committee on the Ethics of Animal Experiments of the Zhejiang Ocean University (Permit Number: 20135107G).

Informed Consent Statement: Not applicable.

Data Availability Statement: The data presented in this study and associated additional data are available upon request.

Acknowledgments: This work was supported by Zhejiang Province Public Technology Application Project of China (No. 2017C33131).

Conflicts of Interest: The authors declare that they have no known competing financial interest or personal relationship that could have appeared to influence the work reported in this paper.

Sample Availability: Samples of the compounds are available from the authors.

References

1. Sanabria, A.; Alvarado, I.; Monge, C. Molecular Pathogenesis of Alzheimer's Disease: An update. *Ann. Neurosci.* **2017**, *24*, 46–54. [[CrossRef](#)]
2. Chaurasiya, N.D.; Leon, F.; Muhammad, I.; Tekwani, B.L. Natural Products Inhibitors of Monoamine Oxidases—Potential New Drug Leads for Neuroprotection, Neurological Disorders, and Neuroblastoma. *Molecules* **2022**, *27*, 4297. [[CrossRef](#)] [[PubMed](#)]
3. Bautista-Aguilera, Ó.M.; Alonso, J.M.; Catto, M.; Iriepa, I.; Knez, D.; Gobec, S.; Marco-Contelles, J. *N*-Hydroxy-*N*-Propargylamide Derivatives of Ferulic Acid: Inhibitors of Cholinesterases and Monoamine Oxidases. *Molecules* **2022**, *27*, 7437. [[CrossRef](#)] [[PubMed](#)]
4. Reitz, C. Genetic Diagnosis and Prognosis of Alzheimer's Disease: Challenges and Opportunities. *Expert Rev. Mol. Diagn.* **2015**, *15*, 339–348. [[CrossRef](#)]
5. Shakir, M.N.; Dugger, B.N. Advances in Deep Neuropathological Phenotyping of Alzheimer Disease: Past, Present, and Future. *J. Neuropathol. Exp. Neurol.* **2022**, *81*, 2–15. [[CrossRef](#)] [[PubMed](#)]
6. Sharma, K. Cholinesterase Inhibitors as Alzheimer's Therapeutics (Review). *Mol. Med. Rep.* **2019**, *20*, 1479–1487. [[CrossRef](#)]
7. Li, Q.; Yang, H.; Chen, Y.; Sun, H.P. Recent Progress in the Identification of Selective Butyrylcholinesterase Inhibitors for Alzheimer's Disease. *Eur. J. Med. Chem.* **2017**, *132*, 294–309. [[CrossRef](#)]
8. Walczak-Nowicka, Ł.J.; Herbet, M. Acetylcholinesterase Inhibitors in the Treatment of Neurodegenerative Diseases and the Role of Acetylcholinesterase in their Pathogenesis. *Int. J. Mol. Sci.* **2021**, *22*, 9290. [[CrossRef](#)]
9. Munir, R.; Ziaur-rehman, M.; Murtaza, S.; Zaib, S.; Javid, N.; Awan, S.J.; Iftikhar, K.; Athar, M.M.; Khan, I. Microwave-assisted Synthesis of (Piperidin-1-yl)Quinolin-3-yl)Methylene)Hydrazine Carbothioamides as Potent Inhibitors of Cholinesterases: A Biochemical and in Silico approach. *Molecules* **2021**, *26*, 656. [[CrossRef](#)]
10. Chung, J.K.; Plitman, E.; Nakajima, S.; Chakravarty, M.M.; Caravaggio, F.; Gerretsen, P.; Iwata, Y.; Graff-Guerrero, A. Cortical Amyloid β Deposition and Current Depressive Symptoms in Alzheimer Disease and Mild Cognitive Impairment. *J. Geriatr. Psychiatry Neurol.* **2016**, *29*, 149–159. [[CrossRef](#)]
11. Javaherian, K.; Newman, B.M.; Weng, H.; Hassenstab, J.; Xiong, C.J.; Coble, D.; Fagan, A.M.; Benzinger, T.; Morris, J.C. Examining the Complicated Relationship Between Depressive Symptoms and Cognitive Impairment in Preclinical Alzheimer Disease. *Alzheimer Dis. Assoc. Disord.* **2019**, *33*, 15–20. [[CrossRef](#)]

12. Chung, J.K.; Plitman, E.; Nakajima, S.; Chakravarty, M.M.; Caravaggio, F.; Takeuchi, H.; Gerretsen, P.; Iwat, Y.; Patel, R.; Mulsant, B.H.; et al. Depressive Symptoms and Small Hippocampal Volume Accelerate the Progression to Dementia from Mild Cognitive Impairment. *J. Alzheimers Dis.* **2016**, *49*, 743–754. [[CrossRef](#)]
13. Lam, C.S.; Li, J.J.; Tipoe, G.L.; Youdim, M.B.H.; Fung, M.L. Monoamine Oxidase A Upregulated by Chronic Intermittent Hypoxia Activates Indoleamine 2,3-Dioxygenase and Neurodegeneration. *PLoS ONE* **2017**, *12*, e0177940. [[CrossRef](#)]
14. Slavich, G.M.; Sacher, J. Stress, Sex Hormones, Inflammation, and Major Depressive Disorder: Extending Social Signal Transduction Theory of Depression to Account for Sex Differences in Mood Disorders. *Psychopharmacol.* **2019**, *236*, 3063–3079. [[CrossRef](#)]
15. Cai, Z. Monoamine Oxidase Inhibitors: Promising Therapeutic Agents for Alzheimer’s Disease (Review). *Mol. Med. Rep.* **2014**, *9*, 1533–1541. [[CrossRef](#)]
16. Behl, T.; Kaur, D.; Sehgal, A.; Singh, S.; Sharma, N.; Zengin, G.; Andronie-Cioara, F.L.; Toma, M.M.; Bungau, S.; Bumbu, A.G. Role of Monoamine Oxidase Activity in Alzheimer’s Disease: An Insight into the Therapeutic Potential of Inhibitors. *Molecules* **2021**, *26*, 3724. [[CrossRef](#)]
17. Nadeem, S.J.; Khan, A.; Kazmi, I.; Rashid, U. Design, Synthesis, and Bioevaluation of Indole Core Containing 2-Arylidine Derivatives of Thiazolopyrimidine as Multitarget Inhibitors of Cholinesterases and Monoamine Oxidase A/B for the Treatment of Alzheimer Disease. *ACS Omega* **2022**, *7*, 9369–9379. [[CrossRef](#)]
18. Quartey, M.O.; Nyarko, J.N.K.; Pennington, P.R.; Heistad, R.M.; Klassen, P.C.; Baker, G.B.; Mousseau, D.D. Alzheimer Disease and Selected Risk Factors Disrupt a Co-regulation of Monoamine Oxidase-A/B in the Hippocampus, but Not in the Cortex. *Front. Neurosci.* **2018**, *12*, 419. [[CrossRef](#)]
19. Ramsay, R.R.; Tipton, K.F. Assessment of Enzyme Inhibition: A Review with Examples from the Development of Monoamine Oxidase and Cholinesterase Inhibitory Drugs. *Molecules* **2017**, *22*, 1192. [[CrossRef](#)]
20. Chu, M.; Chen, X.; Wang, J.; Guo, L.K.; Wang, Q.Q.; Gao, Z.R.; Kang, J.R.; Zhang, M.B.; Feng, J.Q.; Guo, Q.; et al. Polypharmacology of Berberine Based on Multi-Target Binding Motifs. *Front. Pharmacol.* **2018**, *9*, 801–814. [[CrossRef](#)]
21. GBD 2016 Neurology Collaborators. Global, Regional, and National Burden of Alzheimer’s Disease and other Dementias, 1990–2016: A Systematic Analysis for the Global Burden of Disease Study 2016. *Lancet Neurol.* **2019**, *18*, 459–480. [[CrossRef](#)] [[PubMed](#)]
22. Ramsay, R.R.; Majekova, M.; Medina, M.; Valoti, M. Key Targets for Multi-Target Ligands Designed to Combat Neurodegeneration. *Front. Neurosci.* **2016**, *10*, 375–399. [[CrossRef](#)] [[PubMed](#)]
23. Patsenka, A.; Antkiewicz-Michaluk, L. Inhibition of Rodent Brain Monoamine Oxidase and Tyrosine Hydroxylase by Endogenous Compounds-1,2,3,4-Tetrahydroisoquinoline Alkaloids. *Pol. J. Pharmacol.* **2004**, *56*, 727–734. [[PubMed](#)]
24. Bembenek, M.E.; Abell, C.W.; Chrisey, L.A.; Rozwadowska, M.D.; Gessner, W.; Brossi, A. Inhibition of Monoamine Oxidases A and B by Simple Isoquinoline Alkaloids: Racemic and Optically Active 1,2,3,4-Tetrahydro-3,4-Dihydro-, and Fully Aromatic Isoquinolines. *J. Med. Chem.* **1990**, *33*, 147–152. [[CrossRef](#)]
25. Ali, R.; Wahab, A.T.; Wajid, S.; Khan, M.A.; Yousuf, S.; Shaikh, M.; Laghari, G.H.; Rahman, A.U.; Choudhary, M.I. Isolation, Derivatization, in-vitro, and in-silico Studies of Potent Butyrylcholinesterase Inhibitors from *Berberis parkeriana* Schneid. *Bioorganic Chem.* **2022**, *127*, 105944. [[CrossRef](#)]
26. Wan Othman, W.N.N.; Liew, S.Y.; Khaw, K.Y.; Murugaiyah, V.; Litaudon, M.; Awang, K. Cholinesterase Inhibitory Activity of Isoquinoline Alkaloids from three *Cryptocarya* species (Lauraceae). *Bioorg. Med. Chem.* **2016**, *24*, 4464–4469. [[CrossRef](#)]
27. Baek, S.C.; Ryu, H.W.; Kang, M.G.; Lee, H.; Park, D.; Cho, M.L.; Oh, S.R.; Kim, H. Selective Inhibition of Monoamine Oxidase A by Chelerythrine, Anisoquinoline Alkaloid. *Bioorg. Med. Chem. Lett.* **2018**, *28*, 2403–2407. [[CrossRef](#)]
28. Gonzalez, E.P.; Hagenow, S.; Murillo, M.A.; Stark, H.; Suarez, L.C. Isoquinoline Alkaloids from the Roots of *Zanthoxylum rigidum* as Multi-target Inhibitors of Cholinesterase, Monoamine Oxidase A and A β ₁₋₄₂ Aggregation. *Bioorg. Chem.* **2020**, *98*, 103722. [[CrossRef](#)]
29. Fu, Z.Y.; Jin, Q.H.; Xia, Y.N.; Jiang, H.Y.; Guan, L.P. Study on Synthesis and Biological Effects of a Series of 3,4-Dihydroisoquinoline-2(1H)-Carboxamide Derivatives. *Med. Chem. Res.* **2019**, *28*, 52–61. [[CrossRef](#)]
30. Turan-Zitouni, G.; Hussein, W.; Sağlık, B.N.; Tabbi, A.; Korkut, B. Design, Synthesis and Biological Evaluation of novel N-Pyridyl-Hydrazone Derivatives as Potential Monoamine Oxidase (MAO) Inhibitors. *Molecules* **2018**, *23*, 113. [[CrossRef](#)]
31. Chaurasiya, N.D.; Midiwo, J.; Pandey, P.; Bwire, R.N.; Doerksen, R.J.; Muhammad, I.; Tekwani, B.L. Selective Interactions of O-Methylated Flavonoid Natural Products with Human Monoamine Oxidase-A and -B. *Molecules* **2020**, *25*, 5358. [[CrossRef](#)]
32. Knez, D.; Coletti, N.; Iacovino, L.G.; Sova, M.; Pišlar, A.; Konc, J.; Lešnik, S.; Higgs, J.; Kamecki, F.; Mangialavori, I.; et al. Stereoselective Activity of 1-Propargyl-4-Styryl Piperidine-like Analogues that Can Discriminate Between Monoamine Oxidase Isoforms A and B. *J. Med. Chem.* **2020**, *63*, 1361–1387. [[CrossRef](#)]
33. Manzoor, S.; Hoda, N. A Comprehensive Review of Monoamine Oxidase Inhibitors as Anti-Alzheimer’s Disease Agents: A Review. *Eur. J. Med. Chem.* **2020**, *206*, 112787. [[CrossRef](#)]
34. Ellman, G.L.; Courtney, K.; Andres, V.; Featherstone, R.M. A New and Rapid Colorimetric Determination of Acetylcholinesterase Activity. *Biochem. Pharmacol.* **1961**, *7*, 88–95. [[CrossRef](#)]
35. Jalili-Baleh, L.; Babaei, E.; Abdpour, S.; Bukhari, S.N.A.; Foroumadi, A.; Ramazani, A.; Sharifzadeh, M.; Abdollahi, M.; Khoobi, M. A Review on Flavonoid-based Scaffolds as Multi-Target-Directed Ligands (MTDLs) for Alzheimer’s Disease. *Eur. J. Med. Chem.* **2018**, *152*, 570–589. [[CrossRef](#)]

36. Croaker, A.; Davis, A.; Carroll, A.; Liu, L.; Myers, S.P. Understanding of Black Salve Toxicity by Multi-Compound Cytotoxicity Assays. *BMC Complement. Med. Ther.* **2022**, *22*, 247. [[CrossRef](#)]
37. Abd El-Gaber, M.K.; Hassan, H.Y.; Mahfouz, N.M.; Farag, H.H.; Bekhit, A.A. Synthesis, Biological Investigation and Molecular Docking Study of N-Malonyl-1,2-Dihydroisoquinoline Derivatives as Brain Specific and Shelf-Stable MAO Inhibitors. *Eur. J. Med. Chem.* **2015**, *93*, 481–491. [[CrossRef](#)]
38. Ayala, C.E.; Villalpando, A.; Nguyen, A.L.; McCandless, G.T.; Kartika, R. Chlorination of Aliphatic Primary Alcohols via Triphosgene-Triethylamine Activation. *Org. Lett.* **2012**, *14*, 3676–3679. [[CrossRef](#)]
39. Lolaka, N.; Akocaka, S.; Buab, S.; Supuran, C.T. Design, Synthesis and Biological Evaluation of novel Ureido Benzenesulfonamides Incorporating 1,3,5-Triazine Moieties as Potent Carbonic Anhydrase IX Inhibitors. *Bioorg. Chem.* **2019**, *82*, 117–122. [[CrossRef](#)]

Disclaimer/Publisher's Note: The statements, opinions and data contained in all publications are solely those of the individual author(s) and contributor(s) and not of MDPI and/or the editor(s). MDPI and/or the editor(s) disclaim responsibility for any injury to people or property resulting from any ideas, methods, instructions or products referred to in the content.